Fast on-rates allow short dwell time ligands to activate T cells

Christopher C. Govern[a], Michelle K. Paczosa[b], Arup K. Chakraborty[a,c,d,e], and Eric S. Huseby[b,1]

Departments of [a]Chemical Engineering, [c]Chemistry, and [d]Biological Engineering, Massachusetts Institute of Technology, Cambridge, MA 02139; [b]Department of Pathology, University of Massachusetts Medical School, Worcester, MA 01655; and [e]Ragon Institute, Charlestown, MA 02129

Edited by K. Christopher Garcia, Stanford University School of Medicine, Stanford, CA, and accepted by the Editorial Board March 29, 2010 (received for review January 27, 2010)

Two contrasting theories have emerged that attempt to describe T-cell ligand potency, one based on the $t_{1/2}$ of the interaction and the other based on the equilibrium affinity (K_D). Here, we have identified and studied an extensive set of T-cell receptor (TCR)-peptide-MHC (pMHC) interactions for CD4$^+$ cells that have differential K_Ds and kinetics of binding. Our data indicate that ligands with a short $t_{1/2}$ can be highly stimulatory if they have fast on-rates. Simple models suggest these fast kinetic ligands are stimulatory because the pMHCs bind and rebind the same TCR several times. Rebinding occurs when the TCR-pMHC on-rate outcompetes TCR-pMHC diffusion within the cell membrane, creating an aggregate $t_{1/2}$ (t_a) that can be significantly longer than a single TCR-pMHC encounter. Accounting for t_a, ligand potency is K_D-based when ligands have fast on-rates (k_{on}) and $t_{1/2}$-dependent when they have slow k_{on}. Thus, TCR-pMHC k_{on} allow high-affinity short $t_{1/2}$ ligands to follow a kinetic proofreading model.

affinity | kinetic proofreading | MHC | rebinding | T cell receptor

T cell receptors (TCRs) expressed on T cells bind host MHC proteins presenting both self- and foreign pathogen-derived peptides (pMHCs). Depending on the signal emanating from these interactions, diverse biological outcomes ensue. In the thymus, these TCR-pMHC-mediated signals shape the specificity of the mature T-cell repertoire and prevent overtly self-reactive T cells from escaping (1). In the periphery, naive T cells require continual TCR engagement with self-pMHC complexes to receive a homeostatic survival signal, whereas engagements with foreign peptides induce rapid T-cell division and the acquisition of effector functions (2). How T cells interpret the interaction between their TCR and pMHC ligands leading to these different biological outcomes is greatly debated.

Two competing models of T-cell activation have been proposed, with ligand potency being a function of TCR-pMHC equilibrium affinity (K_D) (3–7) or $t_{1/2}$ (8–11). Evidence supporting K_D-based receptor occupancy models of TCR signaling comes from sets of ligands that show a correlation between the K_D and ligand potency (3, 5) and from the fact that ligands induce qualitatively distinct biological outcomes depending on their concentration (12).

In sharp contrast to receptor occupancy models, $t_{1/2}$-based kinetic proofreading models hypothesize that the TCR must be engaged long enough to complete a series of signaling events, including coreceptor recruitment and TCR phosphorylation (13). Increases in the $t_{1/2}$ of the TCR-pMHC engagement raise the probability that any single TCR-pMHC engagement will surpass the threshold amount of time required to initiate T-cell activation (14). Recently, this threshold amount of time has been predicted to be at least 2 s (9, 15). Whether there is, in addition, an optimal $t_{1/2}$ that balances these kinetic proofreading requirements and the serial triggering of TCRs has been debated (16, 17).

Further evidence supporting $t_{1/2}$-based kinetic proofreading models arises from the discovery of antagonist pMHC ligands (18). TCR antagonists induce partial but not complete phosphorylation of the TCR complex and fail to activate T cells fully at any ligand concentration (18). The subsequent discovery that antagonist ligands bind TCRs with a shorter $t_{1/2}$ than stimulatory agonist-pMHC complexes further suggests that activating ligands must engage a specific TCR for a long enough period to allow a series of signaling events to occur (19, 20).

As compelling as the arguments are for $t_{1/2}$ models of T-cell activation, discoveries of highly potent T-cell ligands with a short $t_{1/2}$ suggest that T-cell activation may not be solely dependent on the dwell time (4–6, 21, 22). In an attempt to reconcile why neither K_D nor $t_{1/2}$ fully predicts ligand potency, we have identified low-, medium-, and high-potency T-cell ligands that have medium and fast binding kinetics. The potency of these ligands fails to be described by either a K_D or $t_{1/2}$-based model. By mathematically modeling the biophysical mechanisms leading to T-cell activation using standard assumptions, our results indicate that fast k_{on} allow an individual TCR to bind and rebind rapidly to the same pMHC several times before diffusing away. The rebindings lead to an aggregate $t_{1/2}$ (t_a) that can be significantly longer than individual TCR-pMHC interactions. Importantly, ligand potency correlates closely with this t_a regardless of whether the ligands have fast or slow k_{on} or $t_{1/2}$s. These findings demonstrate that K_D and $t_{1/2}$ models of T-cell activation are not mutually exclusive, because both emerge from a t_a model. In particular, the t_a depends on the $t_{1/2}$ or K_D alone when k_{on} are low or high, respectively. The t_a allows strong K_D/fast-binding kinetic ligands to follow a kinetic proofreading model of activation.

Results

Identification of High, Medium, and Low K_D TCR–pMHC Interactions with Fast Rates of Association and Disassociation. During our previous study of TCRs specific for IA^b/3K, we noticed that several of these TCRs bound IA^b/3K with a strong K_D using very fast binding kinetics (22, 23). However, because some of the k_{off} were exceptionally fast, with loss of all specific binding for some occurring in less than 1 s, the original measurement had a significant error range. Using surface plasmon resonance (SPR) focusing on obtaining TCR-pMHC disassociation rates, we measured the binding kinetics of the B3K506 and B3K508 TCRs interacting with the previously reported and additional IA^b/3K altered peptide ligands (APLs) (Fig. 1).

Although the B3K506 and B3K508 TCRs interact with the IA^b/3K complex with a conventional K_D for agonist ligands (7 μM for the B3K506 and 29 μM for the B3K508), the binding kinetics of the interaction of the B3K506 TCR with IA^b/3K are

Author contributions: C.C.G., A.K.C., and E.S.H. designed research; C.C.G., M.K.P., and E.S.H. performed research; C.C.G. and E.S.H. contributed new reagents/analytic tools; C.C.G., A.K.C., and E.S.H. analyzed data; and C.C.G., A.K.C., and E.S.H. wrote the paper.

The authors declare no conflict of interest.

This article is a PNAS Direct Submission. K.C.G. is a guest editor invited by the Editorial Board.

[1]To whom correspondence should be addressed. E-mail: eric.huseby@umassmed.edu.

This article contains supporting information online at www.pnas.org/lookup/suppl/doi:10.1073/pnas.1000966107/-/DCSupplemental.

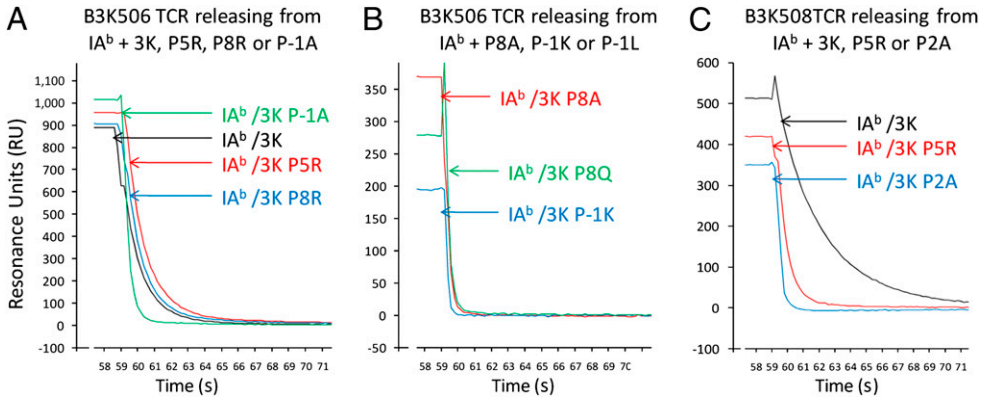

Fig. 1. Release of soluble IA^b/3K and APLs from immobilized B3K506 or B3K508 TCR, monitored SPR. Soluble IA^b/3K, P5R, P8R, or P-1A (*A*); P8A, P5Q, or P-1K loaded onto B3K506 TCRs (*B*); or IA^b/3K, P5R, or P2A loaded onto B3K508 TCRs (*C*) was allowed to disassociate for 60 s at a flow rate of 20 μL/min at 25 °C. Data were collected at 0.2-s intervals and fit to a 1:1 Langmuir binding model to determine the dissociation rate (k_{off}) and $t_{1/2}$ of the MHC/TCR complex. Curves are examples of three independent experiments.

extremely fast: k_{on} = 101,918/M·s and k_{off} = 0.7/s, leading to a $t_{1/2}$ of 0.9 s (Fig. S1 and Table S1). The K_Ds of other B3K506 and B3K508 TCR ligands range from 7–175 μM, all with fast or medium binding kinetics.

B3K506 and B3K508 CD4 T Cells Proliferate in Response to High, Medium, and Low K_D Ligands with a Very Short $t_{1/2}$. To determine the potency of high, medium, and low K_D ligands with differing binding kinetics, mature CD4 T cells from B3K506 and B3K508 Rag1$^{-/-}$ TCR transgenic (Tg) mice were incubated with titrating concentrations of peptides and assessed for proliferation (Fig. 2). Because the peptides with a K_D or $t_{1/2}$ beyond the SPR detection limit failed to induce significant activation, we do not consider them in our subsequent analysis. Of critical importance, except for a 2-fold increase in binding by the 3K P2A peptide to IA^b, the peptides all bind similarly to IA^b proteins (24). Furthermore, mature B3K506 and B3K508 CD4 T cells are equally sensitive to anti-CD3-mediated T-cell signaling, suggesting that the responses of these different T cells to stimulatory ligands can be directly compared (Fig. S2). Our data confirm that fast kinetic ligands can signal, suggesting that the 2-s limit on $t_{1/2}$ is not absolute. Notably, the B3K506 undergoes proliferation at submicromolar peptide concentrations by the 3K, P5R, P8R, and P-1A ligands ($t_{1/2}$ = 0.9, 0.9, 0.8, and 0.3 s, respectively) (Table S1).

Some T-cell ligands with a shorter $t_{1/2}$ than the immunizing ligand can induce superagonist or partial T-cell effector functions if the TCR complex is not efficiently ubiquitinated (18, 25). To determine whether B3K506 and B3K508 T cells undergo complete activation in response to fast kinetic ligands, we chose two additional cellular functions to explore: (*i*) ligand-induced TCR down-regulation as a measure of receptor phosphorylation, ubiquitination, and degradation by Cbl-b (26) and (*ii*) cytokine production by T cells. Consistent with inducing complete phosphorylation of the TCR complex and T-cell activation, fast kinetic ligands induce TCR down-regulation and TNF-α production (Fig. S3 and Table S1).

Ligand Potency of 3K or APLs Fails to Obey Straightforward K_D or $t_{1/2}$ Model. Individually, ligand potency for the B3K506 or B3K508 T cells loosely follows the overall trend of both K_D- and $t_{1/2}$-based models. However, when B3K506 and B3K508 T-cell activation data are compared, neither model suffices (Fig. 3 and Table S1). In regard to K_D, the B3K508 T cells are hyperresponsive. For example, the 3K ligand induces proliferation of B3K506 and B3K508 T cells at a similar nanomolar range concentration, despite having significantly different K_Ds (7 vs. 29 μM). In another example, the B3K506 TCR binds IA^b/P-1A (26 μM) with a similar K_D as the B3K508 TCR binding IA^b/3K (29 μM), yet the B3K506 T cells proliferate at an EC_{50} that is 23-fold less than that of the B3K508 T cells. A failure of K_D to define the ligand potency is further apparent when additional 3K APLs are tested (Fig. 3*A* and Table S1).

In reverse correlation from K_D, ligand potency does not correlate with $t_{1/2}$ because the B3K506 T cells are hyperresponsive.

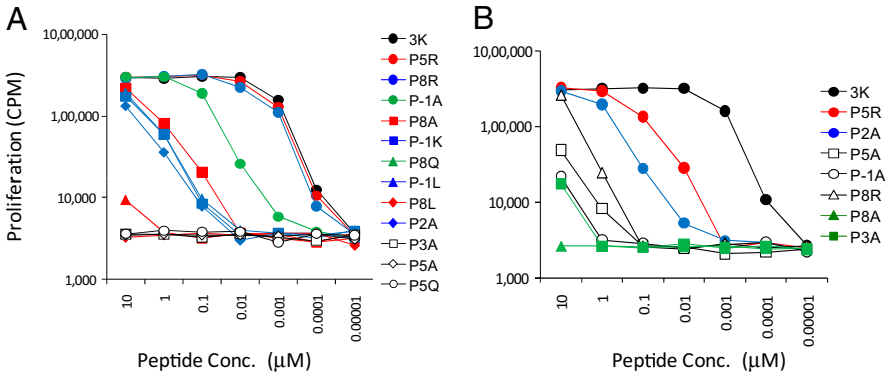

Fig. 2. Activation of 3K-reactive T cells to differing K_D ligands. B3K506 (*A*) and B3K508 (*B*) T cells proliferate when challenged with 3K and APLs. 3K APLs are listed next to each panel by decreasing K_D. Data are representative of at least three independent experiments.

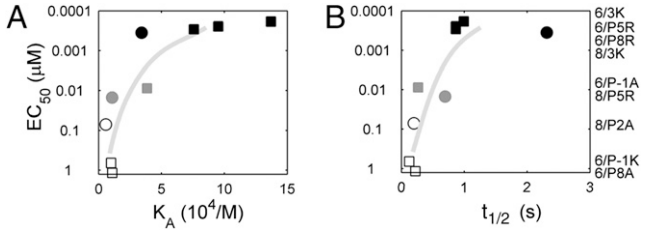

Fig. 3. Failure of K_D or $t_{1/2}$-based models to predict ligand potency. EC_{50} values, based on proliferation, are shown with respect to K_A (*A*) and $t_{1/2}$ (*B*). Data points are labeled by T cell, B3K506 (squares) or B3K508 (circles) and grouped by ligand potency: highest (black), intermediate (gray), and lowest (white). Specific TCR-pMHC pairs are listed to the right, ordered according to EC_{50}. The EC_{50} values are averaged over three measurements.

The 3K ligand induces similar proliferation of the B3K506 T cells ($t_{1/2}$ = 0.9 s) as the B3K508 T cells ($t_{1/2}$ = 2.2 s) (Table S1). In addition, the P5R ligand is significantly less potent in activating the B3K508 T cells than the 3K ligand is in activating the B3K506 T cells, despite having a similar $t_{1/2}$ (0.7 and 0.9 s, respectively). Multiple discrepancies can be observed when comparing other 3K APLs (Fig. 3*B* and Table S1). The finding that each T cell in isolation loosely follows both K_D- and $t_{1/2}$-based models appears to be an artifact of limited variation in the kinetics among the ligands for each T cell. A failure of K_D or $t_{1/2}$ to predict ligand potency is true for cytokine production as well, suggesting that the proliferation response is not anomalous (Fig. S3 and Table S1).

Consistently, activating ligands for B3K506 T cells use a fast k_{on} or strong K_D to compensate for a short $t_{1/2}$. (Because there is a simple relation among them, only two of the three parameters describing the interaction are independent.) Vice versa, B3K508 T cells compensate for a weak K_D by engaging IA^b/3K ligands for a longer $t_{1/2}$. These results suggest that ligand potency is determined by an interplay between the TCR-pMHC k_{on} and $t_{1/2}$ (or K_D and $t_{1/2}$) in a way that allows for enhanced signaling by fast kinetic ligands.

Does a Combined $K_D/t_{1/2}$ Model or Serial Triggering Predict T-Cell Ligand Potency? In an attempt to reconcile how the interplay of K_D and binding kinetics influences T-cell activation, we evaluated whether straightforward merging of the two predicts ligand potency. A combined K_D and $t_{1/2}$ model suggests that increasing the frequency or total number of TCRs engaged by pMHCs would stochastically result in an increase in the number of uncharacteristically long TCR-pMHC interactions. To test this, we identified the change in receptor occupancy required for a strong K_D fast kinetic ligand to be bound to an equal number of TCRs, on average, for at least 2 s as compared with a medium kinetic medium K_D ligand.

To approximate how frequently each pMHC ligand is bound to a TCR, we assume that a quasiequilibrium between TCRs and pMHCs occurs on the time scale of cell-cell contact and that TCRs are far in excess of the relevant pMHCs. The probability that a pMHC is bound to a TCR then depends on the equilibrium association affinity (K_A) through a simple saturation curve (3):

$$\frac{c_{pMHC-TCR}}{c^0_{pMHC}} = \frac{K_A c^0_{TCR}}{1 + K_A c^0_{TCR}} \qquad [1]$$

The parameter c^0_{pMHC} denotes the concentration of pMHCs on the antigen presenting cell (APC), c^0_{TCR} denotes the concentration of TCRs in the interface, and $c_{pMHC\text{-}TCR}$ denotes the concentration of bound pMHC. c^0_{TCR} was estimated to be 20 TCRs per square micrometer (10,000 TCRs per T cell per 500-μm^2 surface area of a T cell; *SI Text*). Within TCR islands, c^0_{TCR} can be locally much higher (80–430 per square micrometer) (27); however, increasing this value had little effect on our results. To convert the measured K_A of the TCR-pMHC pair in solution to K_A when the TCRs and pMHCs are membrane-bound, we have used a confinement length measured for the 2B4 TCR interacting with the MCC88-103 ligand (1.2 nm, corresponding to a conversion factor of 0.262 nm) (8).

The TCR-pMHC saturation curve from Eq. **1** contains a threshold K_D, K^*, above which pMHC ligands are bound at least 50% of the time. Using the above approximations, K^* is 130 μM and pMHC ligands with a 43-μM K_D are bound 75% of the time (Fig. 4). These values mirror measurements made by Grakoui et al. (8), in which the majority of a 60-μM K_D pMHC ligand was bound to a TCR when located within the interface of T cells and APCs. As a result of ligand saturation, strengthening K_D above 100 μM has only a modest effect on the overall frequency of TCRs bound to pMHCs. This saturation curve can be used to show that changes in TCR-pMHC occupancy do not describe ligand potency (*SI Text*).

By comparing ligands with similar EC_{50}s of proliferation yet different $t_{1/2}$s, we tested whether a merged $K_D/t_{1/2}$ model describes ligand potency. Specifically, the tests evaluate whether a stronger K_D for the B3K506 TCR engaging the pMHC generates enough additional bindings to overcome the lower probability of the bindings being long-lived. One comparison is the B3K506 TCR interacting with 3K/P-1A peptide (K_D = 26 μM, $t_{1/2}$ = 0.3 s, EC_{50} = 9 nM) and the B3K508 TCR interacting with the 3K/P5R peptide (K_D = 93 μM, $t_{1/2}$ = 0.7 s, EC_{50} = 15 nM). Assuming that TCRs bind pMHCs with exponentially distributed dwell times, the B3K506 TCR would have to bind 26-fold more IA^b/P-1A ligand than the B3K508 TCR binding IA^b/P5R to generate an equal number of 2-s engagements. However, the 3.6-fold difference in K_D between the two TCR-pMHC pairs leads to only a 1.5-fold difference in receptor occupancy. The effect is qualitatively similar for other comparisons (Fig. S4*A*) and is largely robust to assumptions about the parameters (*SI Text*). Thus, a merged $K_D/t_{1/2}$ model does not properly account for ligand potency. Based on similar reasoning, the effects of serial triggering cannot contribute significantly to ligand potency (Fig. S4 *B* and *C* and *SI Text*). It appears that the roles of the k_{on} and K_D in our data are not to increase the number of bindings, either at any given time (receptor occupancy) or over time (serial triggering).

Could Rebinding of TCRs to pMHCs Expand the Dwell Time for Fast Kinetic Ligands? The failure of K_D, $t_{1/2}$, or serial triggering models indicates that other mechanisms must underlie ligand potency.

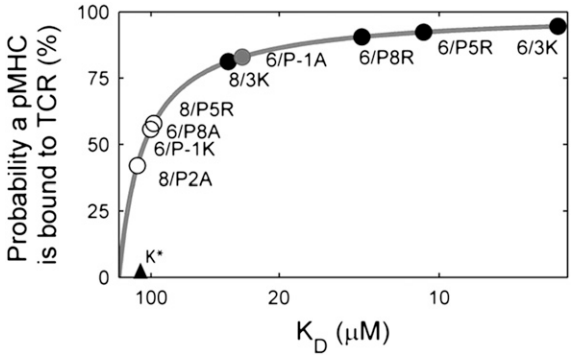

Fig. 4. Receptor occupancy depends only weakly on K_D for pMHC ligands with a K_D stronger than 130 μM. The receptor occupancy predicted by Eq. **1** is plotted, according to the parameter estimates in the text, on a scale that is linear in K_A ($1/K_D$). The predictions for the actual pMHC-TCR pairs in our experiments are superimposed on the plot (circles), colored (black, gray, or white) according to their actual activity as described in the legend for Fig. 3.

The hypothesis of serial triggering, that individual pMHCs can sequentially bind multiple TCRs, led us to wonder whether a pMHC can bind multiple times to the same TCR. The ability of a receptor/ligand pair to associate, disassociate, and reassociate in a finite amount of time before complete disengagement is termed "rebinding." Although TCR-pMHC interactions are usually thought of as single binding events, it is theoretically possible that ligands with fast k_{on} may be able to rebind TCRs (28), especially because they are bound on membranes on which diffusivities are typically slower than in solution. If it occurred, TCR-pMHC rebinding would generate an aggregate dwell time (t_a) of interaction, assuming that the rebindings occur faster than the TCR signaling complex disassembles.

To investigate whether TCR-pMHC rebindings are plausible, we have followed an extensive set of work analyzing diffusion-influenced reactions (29, 30). Our approach has been to apply the particular estimate of the t_a, including rebindings, as provided by Bell (31), because of its simplicity and to suggest that the qualitative results are robust to the choice of model (see below and *SI Text*). In applying Bell's model (31), we assume that pMHCs and TCRs move purely diffusively on flat stiff membranes. Neglecting membrane forces is potentially in conflict with emerging work indicating the role of the actin cytoskeleton in breaking TCR-pMHC bonds, decreasing their $t_{1/2}$ (32). However, when k_{on} are fast enough for rebinding to occur, they happen very quickly; thus, it is unclear how much membrane forces could intervene.

The model also assumes that all rebindings occur at the same rate, which neglects any stabilization of binding that may be provided by coreceptors. Stabilization would have the effect of increasing the propensity of rebinding. Furthermore, the model counts only those rebindings that occur almost immediately, before the TCR and pMHC separate by more than a molecular length scale (e.g., 100 Å), on the order of 1 ms using the parameters below. Although the molecular details of TCR activation are not entirely understood (33, 34), TCR activation is not expected to be appreciably reversed on such short time scales.

Within this framework, Bell's result (31) for the total dwell time, summing the duration of any rebindings that occur, is:

$$t_a = t_{1/2} + \left[\frac{\ln(2)}{2\pi(D_{TCR} + D_{pMHC})}\right] \cdot K_A \qquad [2]$$

The parameters D_{TCR} and D_{pMHC} represent the diffusivities of TCR and pMHC, respectively. From Bell's result (31), it can be seen that the t_a is dependent on the individual $t_{1/2}$ and K_D. The first term in Eq. **2** accounts for the duration of the first binding, whereas the second affinity-dependent term accounts for any subsequent rebindings. Noting that every individual binding event lasts, on average, as long as any other, the expected number of rebindings between a particular pMHC-TCR pair is:

$$\bar{N} = \frac{k_{on}}{2\pi(D_{pMHC} + D_{TCR})} \qquad [3]$$

The parameter k_{on} denotes the on-rate of the pair on the membrane. The system has qualitatively different dependence on $t_{1/2}$ and K_D when k_{on} are small and large. When k_{on} are fast relative to the diffusion rates, pMHC binds and rebinds the same TCR many times, reaching a quasiequilibrium before diffusing away. As a result, the K_D dominates the duration of the interaction when k_{on} are high. However, when k_{on} are slow, rebinding does not occur and $t_{1/2}$ dominates. Because Eq. **2** can be independently motivated by simple arguments such as these, it is qualitatively robust to the choice of model (*SI Text*).

More generally, Eq. **3** suggests that there is a threshold k_{on} above which rebindings are relevant:

$$k^*_{on} = 2\pi(D_{TCR} + D_{pMHC}) \qquad [4]$$

Whenever the k_{on} exceeds this threshold (Eq. **4**; also known as the diffusion-limited rate), at least one rebinding is expected to occur. Importantly, the specific parameter values are important only insofar as they influence this threshold and not the underlying biophysical event (Figs. S5 and S6).

Rebinding of TCRs to pMHCs Uniquely Explains How Fast Kinetic Ligands Induce T-Cell Activation. To evaluate whether rebinding could have an impact on the dwell time of B3K506 or B3K508 TCRs engaging pMHC ligands, we applied Eq. **2** to our dataset. The diffusivities for a TCR and pMHC were estimated at 0.04 and 0.02 $\mu m^2/s$, respectively, corresponding to midrange measured values (*SI Text*). On-rates measured using SPR were converted to k_{on} on the membrane by assuming (*i*) that k_{off} of membrane-bound TCRs binding pMHCs are identical to SPR measurements and (*ii*) that the K_Ds of membrane-bound TCRs engaging pMHCs are proportional to SPR-measured affinities, as done in our analysis of receptor occupancy. Because of limited data, it is generally difficult to convert SPR-measured k_{on} directly to k_{on} on the membrane (35, 36). We discuss sensitivity to the assumptions in *SI Text*.

Using these parameter values, rebinding likely occurs for TCR-pMHC pairs with fast binding kinetics (Fig. 5). Specifically, this initial model predicts that the threshold on-rate for rebinding is 60,000/M·s. As a result, the expected number of rebindings increases from almost none to 1.7 as the on-rate increases in our sample from 11,000/M·s to 102,000/M·s. Because T-cell activity is generally thought to be very sensitive to $t_{1/2}$, a factor of 2 or 3 can be important. When rebindings are accounted for, the highly potent B3K506 T-cell ligands 3K, P5R, and P8R change from a $t_{1/2}$ of 0.9 or 0.8 s to t_as of 2.7, 1.9, and 1.8 s and the medium potent P-1A ligand converts from a $t_{1/2}$ of 0.27 s to a t_a of 0.72 s. Importantly, the t_a is significantly better at predicting ligand potency than the K_D or $t_{1/2}$ (Fig. 6*C* and Figs. S4, S7, and S8).

Within the dataset, two groups of high- or medium-potency ligands arise from different TCR-pMHC binding parameters (Table S1). Using these groups, the competing models can be quantitatively evaluated. The four high-potency ligands (3K, P5R, and P8R binding the B3K506 TCR and 3K binding the B3K508 TCR) have K_Ds and $t_{1/2}$s that vary widely by factors of 4.0 and 2.7, but t_as that vary only by a factor of 1.5 (Fig. 6*C*). The two ligands in the second most potent group (B3K506 TCR binding P2A and B3K508 TCR binding P5R) have K_Ds and $t_{1/2}$s that vary by factors of 3.6 and 2.6, respectively, but t_as that are almost identical, varying only by a factor of 1.1.

Although our t_a model was generated without empirically fitting the data, our estimate for the rebinding threshold, 60,000/M·s, is near the best fit for minimizing the variation in the t_as of the most potent group of ligands (Fig. S5). Quite similarly, for the medium-potent ligands, the best-fit threshold is 45,000/M·s (Fig. 6*D*). Convergence of the t_a model with empirical data suggests that the assumptions and underlying biophysical process are correct.

Discussion

Binding of two proteins is governed by the K_D, k_{on}, and $t_{1/2}$, any two of which suffice to describe the interaction because the three are simply related. Although ligand potency could be dependent on each of these binding characteristics, research over the past two decades has suggested that only the K_D or $t_{1/2}$ matters. Mechanistically, these two mutually exclusive models have been interpreted to mean that T cells are either (*i*) sensitive to the number of TCRs simultaneously bound to pMHC (3–6) or (*ii*) sensitive to ligands that produce a long enough interaction to phosphorylate the TCR complex fully (8–11, 13). In seeming

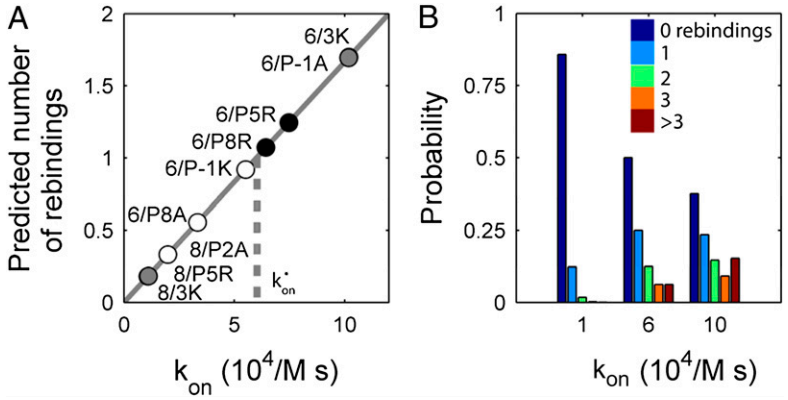

Fig. 5. Fast k_{on} lead to rebinding. (*A*) Average number of rebindings predicted by Eq. **3** is plotted vs. the k_{on}. The threshold for rebinding, k_{on}*, separates pairs expected to rebind at least once from those that rarely rebind. (*B*) Probability of zero, one, two, three, or more than three rebindings between TCRs and pMHCs, according to their on-rate, as predicted from Eq. **2** (*SI Text*).

contradiction to both theories, data presented here suggest that neither the K_D nor $t_{1/2}$ determines the potency of T-cell ligands.

A plethora of data suggests that T cells are increasingly sensitive to long-lived TCR-pMHC engagements, with a $t_{1/2}$ of 2 s being near the shortest allowable time (9, 15). Additionally, T-cell responses are dependent on ligand concentration, suggesting that T cells are also responsive to the frequency of these long-lived bonds. With this as a starting point, we asked how changes in the k_{on} or K_D might allow T cells to be equally reactive to ligands with a different $t_{1/2}$. The IA^b/3K model system is particularly well suited for this analysis because each of the 3K APLs binds IA^b similarly and a relatively large number of TCR-IA^b/3K APL pairs contain several that have similar potency, although using different K_Ds and binding kinetics. These controlled combinations of T cells and pMHC ligands allowed a direct comparison of the different theories of T-cell activation.

Because high-potency T-cell ligands with short $t_{1/2}$s all have fast k_{on}, we hypothesized that TCR-pMHC interactions may be influenced by diffusion rates. Although rebinding is potentially relevant for any binding event, it will be less important for cytosolic reactions because diffusivities in the cytoplasm are relatively high (31). However, when both the receptor and ligand are anchored on membranes, the rates of diffusion are drastically reduced. A recent study of the interaction between membrane-bound CD2 and CD58 using fluorescence recovery after photobleaching (FRAP) suggests that the fast-binding pair may rebind 100 times before separating, significantly increasing the duration of the bonds (37) and potentially explaining the pair's physiological activity (38).

Modeling TCR-pMHC interactions when both are membrane-bound shows that fast k_{on} allow rebinding to occur. Depending on the k_{on}, this effect can greatly extend bond durations, allowing medium-potency ligands with measured $t_{1/2}$s of 0.3 and 0.7 s to generate a t_a near 1 s. As an independent example, the lymphocytic choriomeningitis virus-specific P14 TCR has been shown to bind its cognate H-$2D^b$-gp33 ligand with a low $t_{1/2}$ of 0.7 s (21). Because of a fast k_{on} of 400,000/M·s, our rebinding model predicts that the P14 TCR would have a t_a of 5.5 s, which is fully consistent with kinetic proofreading models of activation.

Most importantly, a rebinding-mediated t_a uniquely predicts ligand potency for B3K506 and B3K508 T cells (Fig. 6). Although our data initially appear to be in conflict with both K_D- and $t_{1/2}$-based activation models, the t_a model is consistent with reports that either $t_{1/2}$ or K_D can be the better predictor of ligand potency. T-cell ligands with slow k_{on} are predicted to follow a strict $t_{1/2}$-based reactivity pattern because rebinding does not occur and the t_a is equal to the $t_{1/2}$ of a single binding event. The canonical $t_{1/2}$-dependent systems, such as the 2B4-IE^k/MCC and 3L.2-IE^k/Hb TCR-pMHC pairs, have slow k_{on} compared with the rebinding threshold we have estimated (45,000–60,000/M·s) (10, 11). Because most T-cell activation studies have been done using these systems, $t_{1/2}$-based models have appeared sufficient and rebindings have not been required to understand ligand potency. For example, the k_{on} for the $t_{1/2}$-dependent 2B4/MCC system studied by Krogsgaard et al. (10) are all less than 6,670/M·s, such that almost no rebindings (<0.15) are predicted to occur.

In contrast to the canonical $t_{1/2}$ models, most T-cell activation studies suggesting that K_D is a better predictor of ligand potency have k_{on} larger than or close to the rebinding threshold (5, 6). Our data suggest that these correlations with K_D occur because

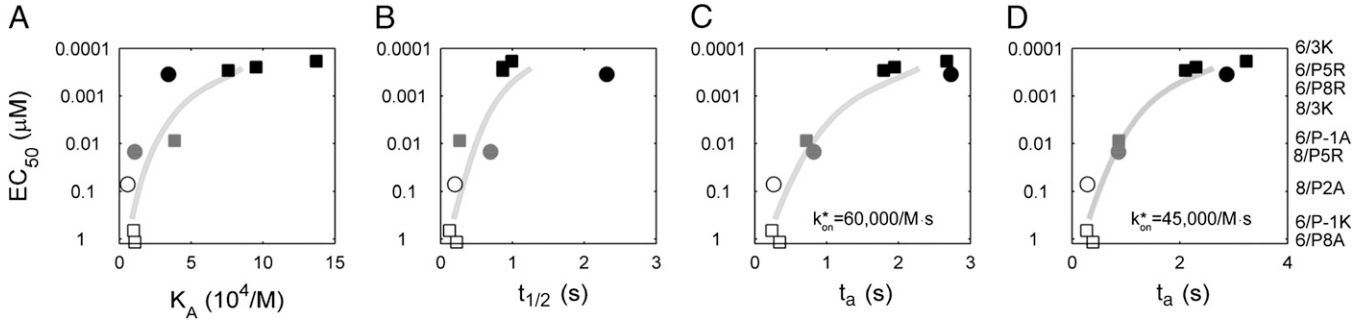

Fig. 6. The t_a is the best predictor of ligand potency for 3K-reactive T cells. EC_{50} values, based on proliferation, are shown with respect to K_D (*A*), $t_{1/2}$ (*B*), and t_a (*C*), with the rebinding threshold set at 60,000/M·s, and (*D*) t_a, with rebinding threshold set at 45,000/M·s.

of rebinding. For example, the K_D dependence of the two peptides studied by Ely et al. (6) is consistent with a dependence on the t_a, with the more potent peptide having a 14-fold faster k_{on} and a predicted 1.3- to 1.4-fold longer t_a according to our model. Thus, observations that ligand potency is dependent on K_D or $t_{1/2}$ are not in conflict with each other; rather, they are different manifestations of the interaction between the T cell and APC when the k_{on} is very fast or very slow. With the continuing emergence of T-cell ligands with very fast k_{on} (4), our findings are likely to have an impact on a large repertoire of T cells.

On completion of this work, we have become aware of results for $CD8^+$ T cells that are in harmony with our conclusions (39).

Materials and Methods

C57BL/6 mice were purchased from the Jackson Laboratory. $Rag1^{-/-}$ B3K506 and $Rag1^{-/-}$ B3K508 TCR Tg mice have been previously described (22). All mice were maintained in a pathogen-free environment in accordance with institutional guidelines in the Animal Care Facility at the University of Massachusetts Medical School. Peptides were purchased from the Medical Research Council at the National Jewish Medical Center. Additional details are provided in *SI Materials and Methods*.

ACKNOWLEDGMENTS. This work was supported by a Beckman Young Investigator and Searle Scholars Award (to E.S.H.), a National Institutes of Health Pioneer Award (to A.K.C.), a National Institutes of Health Biotechnology Training Program grant (to C.C.G.), and National Institutes of Health Grant 1P01AI07/1195/01. E.S.H. is a member of the University of Massachusetts Diabetes Endocrinology Research Center (Grant DK32520).

1. Palmer E (2003) Negative selection—Clearing out the bad apples from the T-cell repertoire. *Nat Rev Immunol* 3:383–391.
2. Tanchot C, Lemonnier FA, Pérarnau B, Freitas AA, Rocha B (1997) Differential requirements for survival and proliferation of CD8 naïve or memory T cells. *Science* 276:2057–2062.
3. Sykulev Y, Cohen RJ, Eisen HN (1995) The law of mass action governs antigen-stimulated cytolytic activity of $CD8^+$ cytotoxic T lymphocytes. *Proc Natl Acad Sci USA* 92:11990–11992.
4. Stone JD, Chervin AS, Kranz DM (2009) T-cell receptor binding affinities and kinetics: Impact on T-cell activity and specificity. *Immunology* 126:165–176.
5. Tian S, Maile R, Collins EJ, Frelinger JA (2007) CD8+ T cell activation is governed by TCR-peptide/MHC affinity, not dissociation rate. *J Immunol* 179:2952–2960.
6. Ely LK, et al. (2005) Antagonism of antiviral and allogeneic activity of a human public CTL clonotype by a single altered peptide ligand: Implications for allograft rejection. *J Immunol* 174:5593–5601.
7. Alam SM, et al. (1996) T-cell-receptor affinity and thymocyte positive selection. *Nature* 381:616–620.
8. Grakoui A, et al. (1999) The immunological synapse: A molecular machine controlling T cell activation. *Science* 285:221–227.
9. Qi SY, Krogsgaard M, Davis MM, Chakraborty AK (2006) Molecular flexibility can influence the stimulatory ability of receptor-ligand interactions at cell-cell junctions. *Proc Natl Acad Sci USA* 103:4416–4421.
10. Krogsgaard M, et al. (2003) Evidence that structural rearrangements and/or flexibility during TCR binding can contribute to T cell activation. *Mol Cell* 12:1367–1378.
11. Kersh GJ, Kersh EN, Fremont DH, Allen PM (1998) High- and low-potency ligands with similar affinities for the TCR: The importance of kinetics in TCR signaling. *Immunity* 9: 817–826.
12. Ashton-Rickardt PG, et al. (1994) Evidence for a differential avidity model of T cell selection in the thymus. *Cell* 76:651–663.
13. McKeithan TW (1995) Kinetic proofreading in T-cell receptor signal transduction. *Proc Natl Acad Sci USA* 92:5042–5046.
14. George AJT, Stark J, Chan C (2005) Understanding specificity and sensitivity of T-cell recognition. *Trends Immunol* 26:653–659.
15. Altan-Bonnet G, Germain RN (2005) Modeling T cell antigen discrimination based on feedback control of digital ERK responses. *PLoS Biol* 3:1925–1938.
16. Kalergis AM, et al. (2001) Efficient T cell activation requires an optimal dwell-time of interaction between the TCR and the pMHC complex. *Nat Immunol* 2:229–234.
17. Holler PD, Kranz DM (2003) Quantitative analysis of the contribution of TCR/pepMHC affinity and CD8 to T cell activation. *Immunity* 18:255–264.
18. Sloan-Lancaster J, Allen PM (1996) Altered peptide ligand-induced partial T cell activation: Molecular mechanisms and role in T cell biology. *Annu Rev Immunol* 14: 1–27.
19. Alam SM, et al. (1999) Qualitative and quantitative differences in T cell receptor binding of agonist and antagonist ligands. *Immunity* 10:227–237.
20. Lyons DS, et al. (1996) A TCR binds to antagonist ligands with lower affinities and faster dissociation rates than to agonists. *Immunity* 5:53–61.
21. Boulter JM, et al. (2007) Potent T cell agonism mediated by a very rapid TCR/pMHC interaction. *Eur J Immunol* 37:798–806.
22. Huseby ES, et al. (2005) How the T cell repertoire becomes peptide and MHC specific. *Cell* 122:247–260.
23. Huseby ES, Crawford F, White J, Marrack P, Kappler JW (2006) Interface-disrupting amino acids establish specificity between T cell receptors and complexes of major histocompatibility complex and peptide. *Nat Immunol* 7:1191–1199.
24. Liu XQ, et al. (2002) Alternate interactions define the binding of peptides to the MHC molecule IA(b). *Proc Natl Acad Sci USA* 99:8820–8825.
25. Cemerski S, et al. (2007) The stimulatory potency of T cell antigens is influenced by the formation of the immunological synapse. *Immunity* 26:345–355.
26. Naramura M, et al. (2002) c-Cbl and Cbl-b regulate T cell responsiveness by promoting ligand-induced TCR down-modulation. *Nat Immunol* 3:1192–1199.
27. Dushek O, Coombs D (2008) Analysis of serial engagement and peptide-MHC transport in T cell receptor microclusters. *Biophys J* 94:3447–3460.
28. Dushek O, Das R, Coombs D (2009) A role for rebinding in rapid and reliable T cell responses to antigen. *PLOS Comput Biol* 5:e1000578.
29. Freeman DL, Doll JD (1983) The influence of diffusion on surface-reaction kinetics. *J Chem Phys* 78:6002–6009.
30. Melo E, Martins J (2006) Kinetics of bimolecular reactions in model bilayers and biological membranes. A critical review. *Biophys Chem* 123:77–94.
31. Bell GI (1978) Models for the specific adhesion of cells to cells. *Science* 200:618–627.
32. Huppa JB, et al. (2010) TCR-peptide-MHC interactions in situ show accelerated kinetics and increased affinity. *Nature* 463:963–967.
33. Davis SJ, van der Merwe PA (2006) The kinetic-segregation model: TCR triggering and beyond. *Nat Immunol* 7:803–809.
34. Call ME, Wucherpfennig KW (2005) The T cell receptor: Critical role of the membrane environment in receptor assembly and function. *Annu Rev Immunol* 23:101–125.
35. Dustin ML, Bromley SK, Davis MM, Zhu C (2001) Identification of self through two-dimensional chemistry and synapses. *Annu Rev Cell Dev Biol* 17:133–157.
36. Robert P, Benoliel AM, Pierres A, Bongrand P (2007) What is the biological relevance of the specific bond properties revealed by single-molecule studies? *J Mol Recognit* 20:432–447.
37. Tolentino TP, et al. (2008) Measuring diffusion and binding kinetics by contact area FRAP. *Biophys J* 95:920–930.
38. Kaizuka Y, Douglass AD, Vardhana S, Dustin ML, Vale RD (2009) The coreceptor CD2 uses plasma membrane microdomains to transduce signals in T cells. *J Cell Biol* 185: 521–534.
39. Aleksic M, et al. (2010) Dependence of T cell antigen recognition on T cell receptor-peptide MHC confinement time. *Immunity* 32:163–174.

Supporting Information

Govern et al. 10.1073/pnas.1000966107

SI Materials and Methods

T-Cell Proliferation. T-cell proliferation was assessed by incubating 1×10^5 naive Rag1$^{-/-}$ B3K506 or B3K508 CD4$^+$ T cells for 48 h with 5×10^5 irradiated C57BL/6 spleen cells and titrating amounts of 3K or 3K variant peptides in 200 μL of RPMI, pulsed with 1 microcurie of [^{3}H]thymidine per well for 18 h, harvested, and counted on a Wallac scintillation counter.

TCR Down-Regulation. In total, 1×10^5 B3K506 and B3K508 Rag1$^{-/-}$ CD4$^+$ T cells were incubated with 5×10^4 bone marrow-derived dendritic cells pulsed with titrating amounts of 3K or variant peptides for 16 h in 200 mL of RPMI. Cells were then washed and labeled with anti-TCR-β-FITC (HAM597), anti-CD69-phycoerythrin, anti-CD4-peridinin chlorophyll protein, and anti-Thy1.2-APC. TCR-β expression was assessed by flow cytometry (FACSCalibur; BD Biosciences) on CD4$^+$ Thy1.2$^+$ cells and analyzed using FlowJo version 8.3 (TreeStar).

Intracellular Cytokine Production. In total, 3×10^5 CD4 B3K506 or B3K508 Rag1$^{-/-}$ CD4$^+$ T cells were stimulated with 1×10^5 C57BL/6 bone marrow-derived dendritic cells pulsed with titrating concentrations of 3K or variant peptides in the presence of GolgiPlug (1 μL/mL; BD Biosciences) for 5 h at 37 °C. T cells were then surface-stained with anti-CD4 and anti-CD8, washed, fixed in 4% (vol/vol) formaldehyde (Fischer Scientific), and stained for intracellular TNF-α using a Cytofix/Cytoperm kit (BD Biosciences) in accordance with the manufacturer's protocol. TNF-α expression was assessed by flow cytometry (FACSCalibur) on CD4$^+$ T cells and analyzed using FlowJo version 8.3.

SPR Measurements of TCR-pMHC Kinetics and Affinities. Soluble IA^b/3K and IA^b/3K peptide variants were expressed and produced using the baculovirus expression system, as previously described (1, 2). K_Ds and binding kinetics for TCRs binding to IA^b/3K and APLs were obtained on BIAcore 2000 and 3000 instruments (BIAcore AB). Data points were collected at 0.2-s intervals and analyzed with Bioeval 4.1 software (BIAcore AB). Scatchard analyses of the equilibrium data were used to determine the dissociation constant (K_D). The kinetic data were used to determine the dissociation rate (k_{off}) and the association rate (k_{on}) were calculated from the K_D and k_{off} ($k_{on} = k_{off}/K_D$).

Tests of Different Models of Ligand Potency and Sensitivity to Model Parameters. ***Tests to determine whether T-ligand potency correlates with TCR-pMHC occupancy when TCRs and pMHCs are membrane-bound.*** T-cell ligand potency does not correlate with the measured K_D (Fig. 3*A*). Even though the K_D measurement of soluble proteins does not describe ligand activity, it is possible that changes in receptor occupancy when TCRs and pMHCs are membrane-bound do describe our data. In this section, we provide an alternate argument against receptor-occupancy (K_D)-based theories. In the main text, we concluded that the affect of K_D on receptor occupancy is weak because of saturation effects (Fig. 4). Thus, for a K_D-based model to explain the wide range of activities seen in our dataset, the effect of receptor occupancy on activity would have to be quite strong.

To assess directly whether changes in receptor occupancy can account for ligand potency, we have compared two quantities: (*i*) the dose–response of a T cell to different concentrations of ligand and (*ii*) the response of the T cell, at fixed concentrations of ligand, to ligands with different K_Ds. Because changes in concentration and K_D lead independently to changes in receptor occupancy, the dose–response curves and the mutation studies provide independent measures of the effect of receptor occupancy on activity. By comparing K_D-based changes in receptor occupancy (comparing different ligands) with concentration-based changes (comparing the same ligand at different concentrations), the impact of K_D can be directly assessed. To do so, we posited that changes in peptide concentration lead directly to changes in receptor occupancy, assuming that TCRs are in great excess and that the additional peptide binds MHC. For example, we assume that a 2-fold increase in peptide concentration leads to a 2-fold increase in pMHC-TCR engagement.

Consonant with our arguments against a pure K_D theory in the main text, the data indicate that the effect of receptor occupancy on activity is not strong enough to explain our data. The dose–response curves indicate that large changes in receptor occupancy are required to increase activity, which are far larger than the difference in receptor occupancies between two peptides with different K_Ds. This can particularly be seen by examining the responses of the B3K506 TCR to two different peptides, IA^b/3K and IA^b/P-1A. The IA^b/3K peptide is more stimulatory for the B3K506 TCR than for the IA^b/P-1A peptide at every concentration of peptide. In particular, at a concentration of 0.0001 μM, the 3K peptide induces 14-fold more proliferation than the P-1A peptide. The 3K peptide also has a stronger K_D (7 and 26 μM, respectively), in apparent agreement with a K_D theory. Its 4-fold higher affinity can lead at most, however, to a 4-fold higher receptor occupancy at each concentration of peptide (Eq. **1**). Because of saturation, the actual increase is probably less. In fact, using estimates of relevant parameters, we predicted in the main text that its receptor occupancy is only 12% higher than the receptor occupancy of the P-1A peptide (Fig. 4).

For the K_D model to explain the differential activity of these two peptides, a 4-fold increase in receptor occupancy must be able to generate a 14-fold increase in proliferation. A 4-fold increase in the concentration of P-1A from 0.0001 μM, however, barely increases its proliferation (2-fold). In fact, the concentration of the P-1A ligand must be increased over 50-fold to recapitulate the activity of the 3K peptide at 0.0001 μM. Even if a 50-fold increase in concentration leads to a smaller increase in receptor occupancy, the gap is quite large.

Because the different affinities in our dataset lead to only small differences in receptor occupancy and peptide activity is not very sensitive to receptor occupancy, K_D theories do not explain our data.

Testing the impact of serial triggering. Because neither K_D nor $t_{1/2}$ models, independently or combined, explained the T-cell activation data, we assessed whether serial triggering could influence ligand potency. The serial triggering hypothesis postulates that an individual pMHC can sequentially trigger multiple distinct TCRs (3, 4). Thus, the faster on-rate of IA^b/3K-binding B3K506 TCRs would lead to a greater number of distinct binding events over the course of the T-cell-APC interaction. Serial triggering of many more TCRs by fast kinetic ligands vs. slow kinetic ligands could lead to an increase in the probability of generating uncharacteristically long-lived interactions.

To test whether serial triggering accounts for the ligand potency of IA^b/3K-reactive T cells, we determined how many more binding events would be required for a strong K_D and fast kinetic ligand to bind an equal number of TCRs for at least 2 s as a medium kinetic and medium K_D ligand. We followed the analysis conducted by Coombs et al. (5). In this model, the number of distinct TCRs bound by a pMHC is as follows:

$$N = \frac{\ln(2)}{t_{1/2}}\left(\frac{K_A c_{TCR}}{1 + K_A c_{TCR}}\right)T$$

The parameter T denotes the total time a pMHC is present in the APC-TCR interface. Because the number of distinct TCRs a pMHC binds depends on the affinity and k_{on} in exactly the same way as the receptor occupancy, the conclusion that serial triggering also does not account for our data is not surprising.

As an example, we compared the responses of the fast kinetic B3K506 TCR binding the IA^b/P-1A ligand and the B3K508 TCR binding IA^b/P5R. These two peptides induce similar activity but have different K_D and binding kinetics. If we assume that TCRs binding pMHC have exponentially distributed dwell times, as in the main text, then to have a similar probability of engaging pMHC for 2 s, the B3K506 TCR would have to generate 26-fold more distinct binding events to the IA^b/P-1A ligand than the B3K508 TCR binding IA^b/P5R. However, the 3.6-fold difference in K_D between the two TCR-pMHC pairs leads to only a 6.5-fold difference in the in number of distinct bound TCRs. The impact of serial triggering on equalizing $t_{1/2}$s becomes worse when a higher $t_{1/2}$ threshold is assumed (Fig. S4*C*), further suggesting that serial triggering cannot lead to significant increases in uncharacteristically long-lived TCR-pMHC interactions. Most importantly, both the B3K506 and B3K508 T cells demonstrate enhanced activity to ligands with increasing $t_{1/2}$. These data indicate that for fast kinetic medium and strong K_D ligands, T-cell activation is negatively correlated with increasing numbers of binding events.

Model and parameter sensitivity analysis. A. Model merging receptor occupancy and dwell time. In the main text, we estimated parameters in Eq. **1** to evaluate whether receptor occupancy and dwell time models could jointly explain our data. Recent arguments suggest that the relevant TCR concentration in Eq. **1** is the effective concentration of TCRs in the synapse, averaged over TCR-rich and TCR-sparse regions, assuming that the TCRs can move freely between the two regions (6). Thus, the concentration of TCRs in the interface between the T cell and APC, c^0_{TCR}, was estimated in the main text by dividing the total number of TCRs on a T cell (10,000 TCRs per T cell) by the total surface area of a T cell (500 μm^2), leading to an estimate of 20 TCRs per square micrometer (7). Within TCR-rich regions (e.g., islands), c^0_{TCR} is locally much higher (80–430 TCRs per square micrometer) (8). Although we have used the lower effective concentration of TCRs, higher concentrations would only improve the robustness of our conclusions, as we demonstrate below.

To convert the measured K_A of TCR-pMHC in solution to K_A when the TCR and pMHC are membrane-bound, we have used a confinement length measured for the 2B4 TCR interacting with the MCC88-103 ligand (1.2 nm, corresponding to a conversion factor of 0.262 nm) (7). Although this conversion has precedent, it is uncertain, as recent research reveals (9, 10). The need for more direct measurements of membrane kinetics has long been acknowledged (11). In particular, one recent study of pMHC-TCR kinetics on the membrane has suggested that k_{on} and k_{off} are faster on the membrane than solution-based measurements suggest and that actin-cytoskeleton-driven membrane motion has a role in tearing apart bonds (10). The role of the membrane in breaking apart bonds as short-lived as those in this study is unclear.

Because the parameters involved in our models are uncertain, we checked to determine if our conclusions were robust to parameter variations. First, we checked the validity of our conclusion that the receptor occupancy is saturated. To do so, we varied the K*, modeling uncertainty both in the concentration of TCRs on the T cell and in likely errors in converting SPR-measured affinities to affinities on the membrane (Fig. S6). If the threshold K_D is weaker than our estimate, even weakly binding peptides will almost always be bound and the conclusion is robust. As the threshold K_D becomes much stronger than our estimate, some of the weaker binding peptides in our sample become unsaturated. Even in these cases, however, it is unlikely that changes in the K_D could compensate for changes in the $t_{1/2}$ in a merged receptor occupancy/dwell time model. The dwell time depends strongly (exponentially) on the $t_{1/2}$, whereas the receptor occupancy depends weakly (sublinearly) on the K_D, even if the system is not saturated (see the arguments in the tests of the pure affinity model).

B. Rebinding. B1. Model sensitivity. In the main text, we applied Bell's model (12) to estimate the importance of rebinding on the membrane. Here, we briefly motivate rebinding models to suggest that our qualitative conclusions are robust to the choice of model.

Once a ligand and receptor debind, we assume that there is some probability they will rebind within a given time interval. Suppose we knew this probability (p). The number of rebindings would then be a geometrically distributed random variable with parameter 1−p, assuming that every rebinding is independent, and the expected number of rebindings would be p/(1−p).

What is the probability p? Clearly, it depends on the time interval over which rebindings are counted. In the case of the interaction between TCRs and pMHCs, we are only interested in those rebindings that occur relatively quickly, before the TCR signaling complex disassembles. Because it is unclear how quickly the TCR signaling complex disassembles, however, models must choose a different measure of "quickness." (Analytically, other measures are also more tractable.) One reasonable approach is to count only those rebindings that occur before the pMHC binds to another TCR for the first time.

In a different approach, Bell's model (12) can be interpreted to count only those rebindings that occur almost immediately, before the receptor and ligand are ever separated by more than a molecular distance. To see this, consider the probability that a pMHC binds to a TCR before diffusing away when it is within a molecular distance of the TCR. For simplicity, we can model the reaction and diffusion as competing exponential processes with rates corresponding to their characteristic rates, which scale as k_{on}/L^2 and D/L^2, respectively, where L is the molecular distance. (Note that k_{on} is expressed on a per molecule basis.) Applying this simple analysis to determine the probability p (13), it is possible to obtain Bell's model (12) (Eq. **2**), within a constant factor.

How sensitive are the conclusions to the particular choice of model? Clearly, the choice of which rebindings to count will affect the quantitative results. Allowing more time for the pMHC and TCR pair to rebind, for example, will lead to larger predictions for the t_a. The qualitative prediction of the model, however, is robust. Independent of the choice of model, the t_a will depend on the $t_{1/2}$ and K_D when k_{on} are low or high, respectively, and on a combination of the two when k_{on} are intermediate. The robustness of this conclusion stems from the fact that it can be motivated independently by simple arguments. When k_{on} are slow, rebinding will not occur and the t_a will depend on the single-interaction $t_{1/2}$. Conversely, when k_{on} are fast, a pMHC and a TCR will rebind many times, essentially equilibrating. As a result, the t_a will depend only on the K_D when k_{on} are large.

B2. Parameter estimates and sensitivity. To evaluate whether rebinding could have an impact on the dwell time of B3K506 or B3K508 TCRs engaging IA^b/3K and APL ligands, we estimated the parameters in Eq. **2**. The diffusivity for a TCR and a pMHC was estimated using published experimental measurements. We used 0.04 and 0.02 $\mu m^2/s$ as typical estimates of the diffusivities of a pMHC (14–16) and a TCR, respectively (17–19). The range of reported diffusivities is from 0.01 to 0.1 $\mu m^2/s$ for pMHCs, with measurements concentrated toward the lower end, and from 0.01 to 0.12 $\mu m^2/s$ for TCRs, although the higher estimates may apply to TCRs outside lipid rafts. We converted our SPR measurements

of k_{on} to k_{on} on the membrane by assuming that affinities on the membrane are proportional to SPR-measured affinities, as in our analysis of receptor occupancy, and, further, by assuming that k_{off} on the membrane are identical to those measured by SPR. Because of limited data, it is generally difficult to convert SPR-measured k_{on} to k_{on} on the membrane (11, 20). A recent study of pMHC-TCR kinetics on the membrane has suggested that k_{on} and k_{off} are faster on the membrane than solution-based measurements suggest and that actin-cytoskeleton-driven membrane motion has a role in tearing apart bonds (10). The role of the membrane in breaking apart bonds as short-lived as those in this study is unclear. Additionally, because faster k_{on} promote rebinding but membrane motion driving the pair apart inhibits rebinding, it is too early to understand how our qualitative results would be affected.

Because of the uncertainty in these parameters, we checked the robustness of our conclusion that rebinding explains the potency of the peptides in our dataset. To do so, we varied the threshold for rebinding, k_{on}*, which models uncertainties in the diffusivities of the TCR and the pMHC and errors in converting SPR-measured k_{on} to k_{on} on the membrane. It is also a rough way of accounting for other factors that might increase or decrease the likelihood of rebinding, such as membrane motion, as well as uncertainty in the model itself. Threefold differences in the threshold k_{on} do not qualitatively affect our conclusions (Figs. S5 and S7). As the threshold for rebinding increases, rebindings become less likely for any given pMHC-TCR pair and the effect of rebinding on the t_a weakens. As long as the rebinding threshold falls within or near the range of k_{on} in our data, it will explain at least part of the difference between the B3K506 and B3K508 TCRs, balancing their K_D and $t_{1/2}$.

Independent of the parameter estimates, we also provided best-fit values in the main text, which, being close to our estimates, reinforced our conclusions. We provide another type of best-fit analysis, based on fitting the models to groups of peptides with similar activity, in Fig. S8 to show this conclusion in another way.

1. Huseby ES, et al. (2005) How the T cell repertoire becomes peptide and MHC specific. *Cell* 122:247–260.
2. Huseby ES, Crawford F, White J, Marrack P, Kappler JW (2006) Interface-disrupting amino acids establish specificity between T cell receptors and complexes of major histocompatibility complex and peptide. *Nat Immunol* 7:1191–1199.
3. Valitutti S, Müller S, Cella M, Padovan E, Lanzavecchia A (1995) Serial triggering of many T-cell receptors by a few peptide-MHC complexes. *Nature* 375:148–151.
4. Wofsy C, Coombs D, Goldstein B (2001) Calculations show substantial serial engagement of T cell receptors. *Biophys J* 80:606–612.
5. Coombs D, Kalergis AM, Nathenson SG, Wofsy C, Goldstein B (2002) Activated TCRs remain marked for internalization after dissociation from pMHC. *Nat Immunol* 3:926–931.
6. Zhu DM, Dustin ML, Cairo CW, Golan DE (2007) Analysis of two-dimensional dissociation constant of laterally mobile cell adhesion molecules. *Biophys J* 92:1022–1034.
7. Grakoui A, et al. (1999) The immunological synapse: A molecular machine controlling T cell activation. *Science* 285:221–227.
8. Dushek O, Coombs D (2008) Analysis of serial engagement and peptide-MHC transport in T cell receptor microclusters. *Biophys J* 94:3447–3460.
9. Tolentino TP, et al. (2008) Measuring diffusion and binding kinetics by contact area FRAP. *Biophys J* 95:920–930.
10. Huppa JB, et al. (2010) TCR-peptide-MHC interactions in situ show accelerated kinetics and increased affinity. *Nature* 463:963–967.
11. Dustin ML, Bromley SK, Davis MM, Zhu C (2001) Identification of self through two-dimensional chemistry and synapses. *Annu Rev Cell Dev Biol* 17:133–157.
12. Bell GI (1978) Models for the specific adhesion of cells to cells. *Science* 200:618–627.
13. DeGroot MH (2002) *Probability and Statistics* (Boston Addison-Wesley) 3rd Ed, p 816.
14. Wade WF, Freed JH, Edidin M (1989) Translational diffusion of class II major histocompatibility complex molecules is constrained by their cytoplasmic domains. *J Cell Biol* 109:3325–3331.
15. Edidin M, Kuo SC, Sheetz MP (1991) Lateral movements of membrane glycoproteins restricted by dynamic cytoplasmic barriers. *Science* 254:1379–1382.
16. Pecht I, Gakamsky DM (2005) Spatial coordination of CD8 and TCR molecules controls antigen recognition by CD8+ T-cells. *FEBS Lett* 579:3336–3341.
17. Sloan-Lancaster J, et al. (1998) ZAP-70 association with T cell receptor zeta (TCRzeta): Fluorescence imaging of dynamic changes upon cellular stimulation. *J Cell Biol* 143: 613–624.
18. Favier B, Burroughs NJ, Wedderburn L, Valitutti S (2001) TCR dynamics on the surface of living T cells. *Int Immunol* 13:1525–1532.
19. Gakamsky DM, et al. (2005) CD8 kinetically promotes ligand binding to the T-cell antigen receptor. *Biophys J* 89:2121–2133.
20. Robert P, Benoliel AM, Pierres A, Bongrand P (2007) What is the biological relevance of the specific bond properties revealed by single-molecule studies? *J Mol Recognit* 20:432–447.

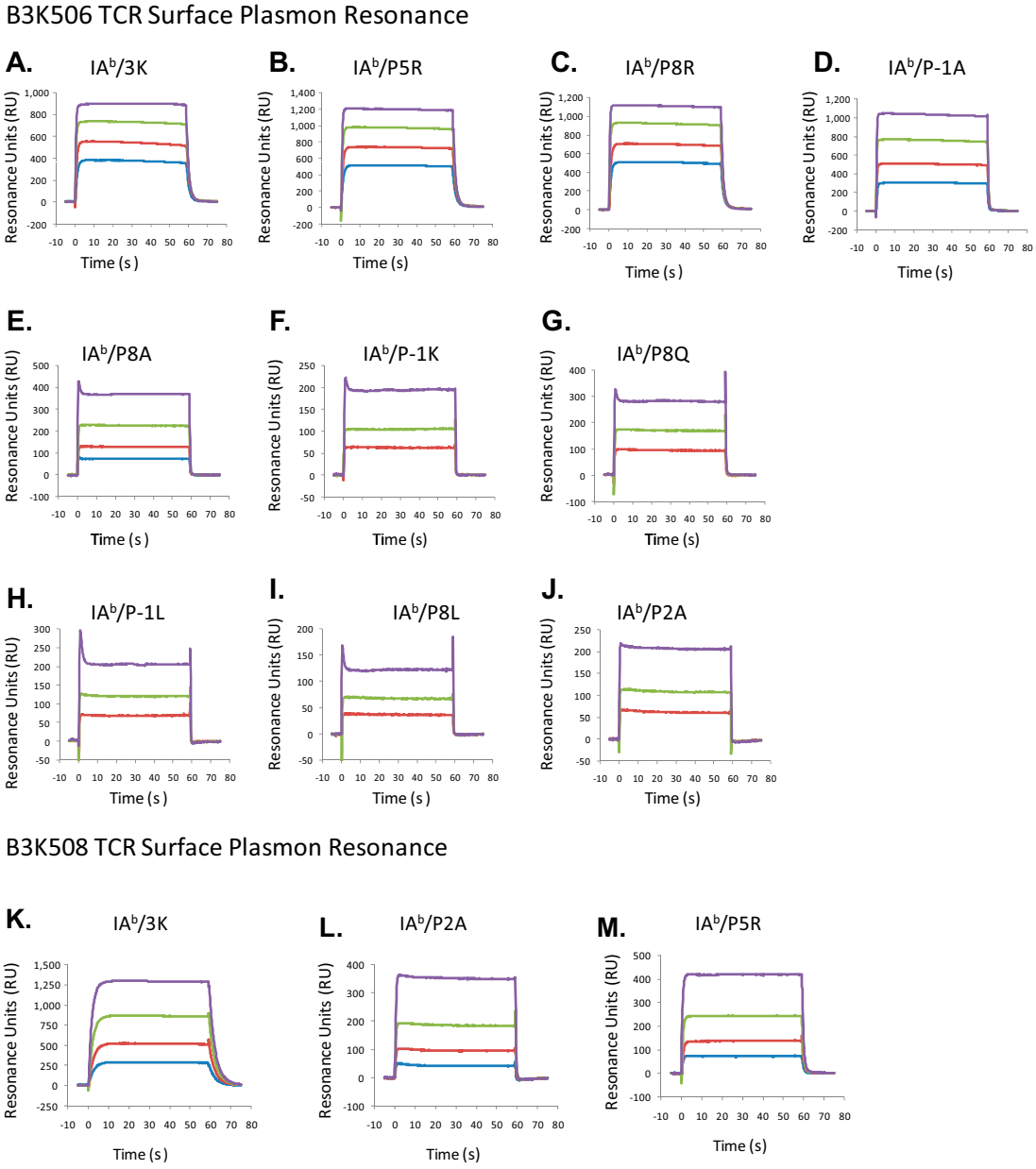

Fig. S1. B3K506 and B3K508 TCRs interact with IA^b/3K and peptide variants with differing rates of association and disassociation. The affinity and kinetics of soluble monomeric IA^b-3K or variant peptide ligands binding to immobilized B3K506 and B3K508 TCRs were analyzed by SPR using BIAcore 2000 and BIAcore 3000 instruments (BIAcore AB). Approximately 2,000 resonance units (RU) of soluble B3K506 TCR was captured on the surface of a CM5 biosensor flow cell by an immobilized anti-Cα mAb, ADO-304. For the B3K506 T cells, soluble IA^b/3K or variant peptides were injected at 20 μL/min for 60 s through a CM5 biosensor flow cell at a concentration of 3K WT (4, 8, 16, and 32 μM) (*A*), P5R (5.6, 11.2, 22.5, and 45 μM) (*B*), P8R (8, 16, 32, and 64 μM) (*C*), P-1A (8, 16, 32, and 64 μM) (*D*), P8A (8, 16, 32, and 64 μM) (*E*), P-1K (12.9, 25.7, and 51.4 μM) (*F*), P8Q (13, 26, and 52 μM) (*G*), P-1L (16, 32, and 64 μM) (*H*), P8L (4, 8, 16, and 32 μM) (*I*), and P2A (4, 8, 16, and 32 μM) (*J*). No specific binding was detected for the P3A, P5A, and P5Q ligands interacting with the B3K506 TCR. For the B3K508 T cells, soluble IA^b/3K or variant peptides were injected at 20 mL/min for 60 s through a CM5 biosensor flow cell at a concentration of 3K WT (4, 8, 16, and 32 μM) (*K*), P5R (5.6, 11.2, 22.5, and 45 μM) (*L*), and P2A (4, 8, 16, and 32 μM) (*M*). Limited binding was detected for the P5A ligand binding the B3K508 TCR at 32 and 64 μM. No specific binding was detected for the P-1A, P8R, P8A, and P3A ligands interacting with the B3K508 TCR. As a control for bulk fluid phase refractive index, the IA^b-3K preparations were also injected through a fourth flow cell with an immobilized irrelevant TCR Ani 2.3 specific for HLA-DR52c. All samples reached equilibrium binding within 10 s. The complex was allowed to dissociate for 60 s between injections. Raw data were corrected for the bulk signal from buffer and IA^b-3K by performing identical injections through a flow cell in which an irrelevant TCR was immobilized. The data were further corrected for the loss of captured TCR during the series of injections based on the observed k_{off} of the TCR from the anti-Cα mAb (~4.5×10^{-4} per second). The data were analyzed with BIAcore Bioeval 4.1 software.

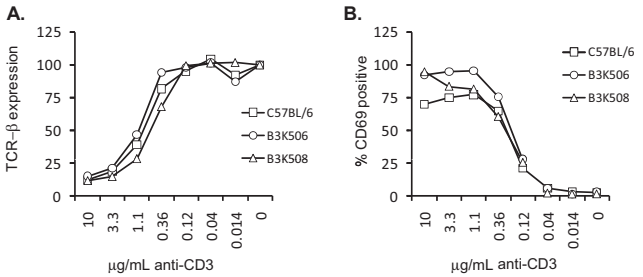

Fig. S2. C57BL/6, B3K506, and B3K508 CD4$^+$ T cells down-regulate TCR expression and up-regulate CD69 expression equivalently in response to titrating amounts of anti-CD3 cross-linking. CD4 T cells were incubated in plates coated with 10 μg/mL anti-CD28, titrating amounts of anti-CD3 for 18 h, and were analyzed by flow cytometry for TCR-β expression (*A*) and CD69 expression (*B*). TCR-β expression is normalized for each T-cell population to the expression at which no activation occurs. Data are the average of three wells per variability and are representative of two independent experiments.

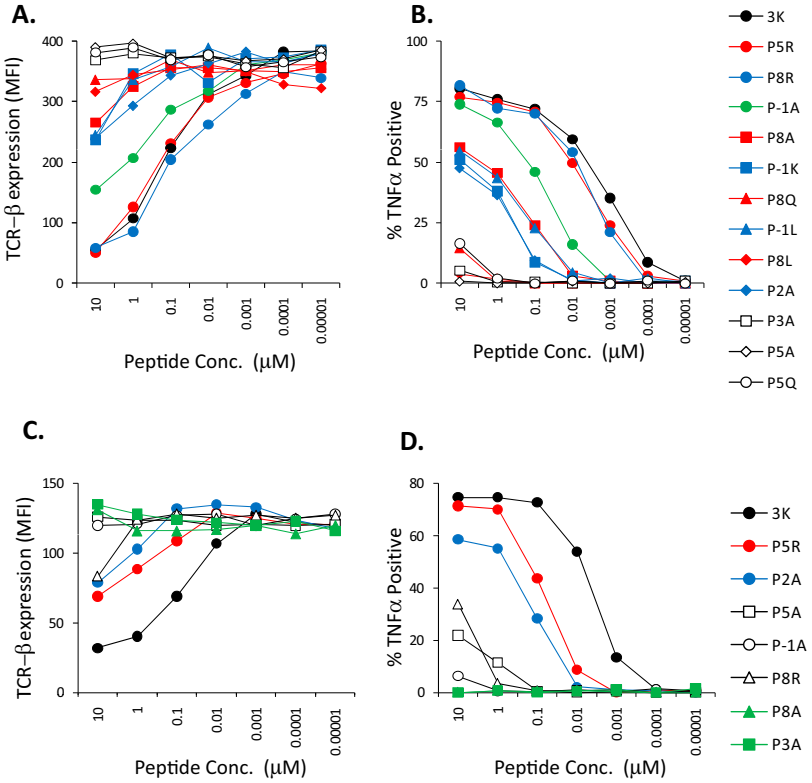

Fig. S3. B3K506 and B3K508 T cells down-regulate TCR expression and produce TNF-α when challenged with high, medium, and low K_D ligands. Naive B3K506 CD4 T cells down-regulate TCR expression (*A*) and produce TNF-α to 3K and APL ligands (*B*). Peptide ligands are listed by decreasing K_D, with the 3K peptide having the strongest K_D and the P5Q peptide having the weakest (undetectable) K_D. Naive B3K508 CD4 T cells down-regulate TCR expression (*C*) and produce TNF-α to 3K and APL ligands (*D*). Peptide ligands are listed by decreasing K_D. Data are representative of at least three independent experiments.

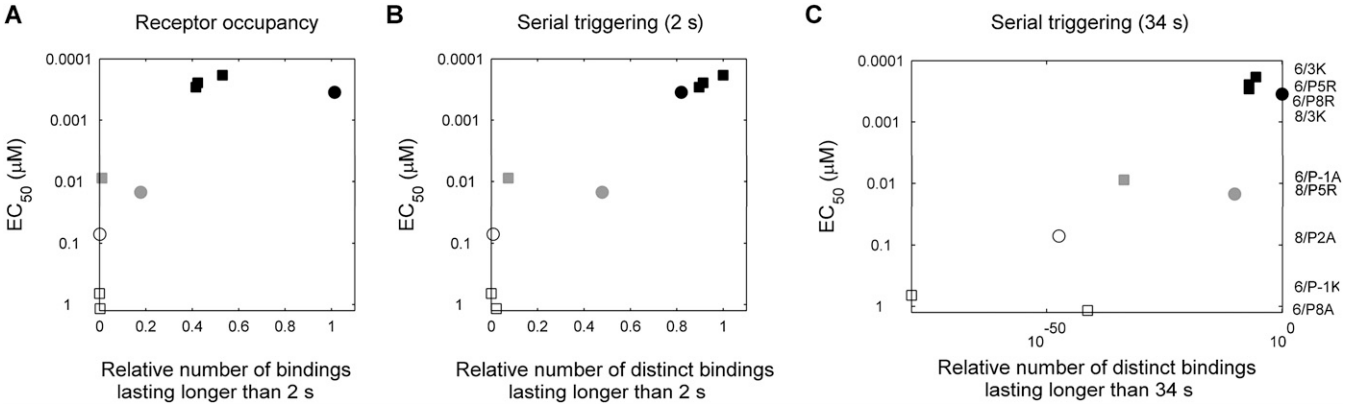

Fig. S4. Evaluating models that correlate ligand potency with the number of long-lived bonds between pMHCs and TCRs. (*A*) Model merging receptor occupancy and dwell time does not explain the activities of the pMHC-TCR pairs. The pMHC-TCR pairs are ranked according to the average number of interactions between them, at any given time, that have lasted longer than 2 s This average number was calculated as the product of two quantities: (*i*) the fraction of peptides bound at any given time, as given in Eq. **1**, and (*ii*) the fraction of such bindings that lasts longer than 2 s, assuming exponentially distributed binding times. The result has been normalized by the B3K508 peptide interacting with the 3K peptide, which is predicted to be the most active. The results are fairly insensitive to the parameter estimates because of the strong (exponential) dependence on the $t_{1/2}$ and the weak (sublinear) dependence on the affinity. (*B* and *C*) Model merging serial triggering and dwell time does not explain the activities of the pMHC-TCR pairs. The pMHC-TCR pairs are ranked according to the number of distinct interactions between them that last longer than a threshold time. The number of interactions is normalized by the number of interactions for the B3K506 TCR interacting with the 3K peptide, which is predicted to be most active. The threshold time required to activate a TCR is assumed to be 2 s (*B*) and 34 s (*C*). (*C*) Note that this panel is on a log scale.

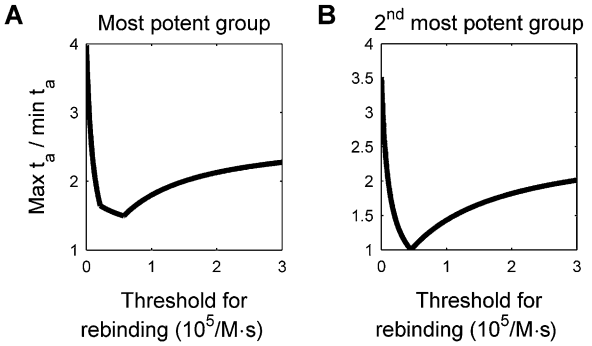

Fig. S5. Determining the optimal rebinding threshold for the data. The variation in t_as within groups of similar activity is plotted against different rebinding thresholds for the most potent group of peptides (*A*) and the second most potent group of peptides (*B*). The optimal thresholds are 60,000/M·s (*A*) and 45,000/M·s (*B*).

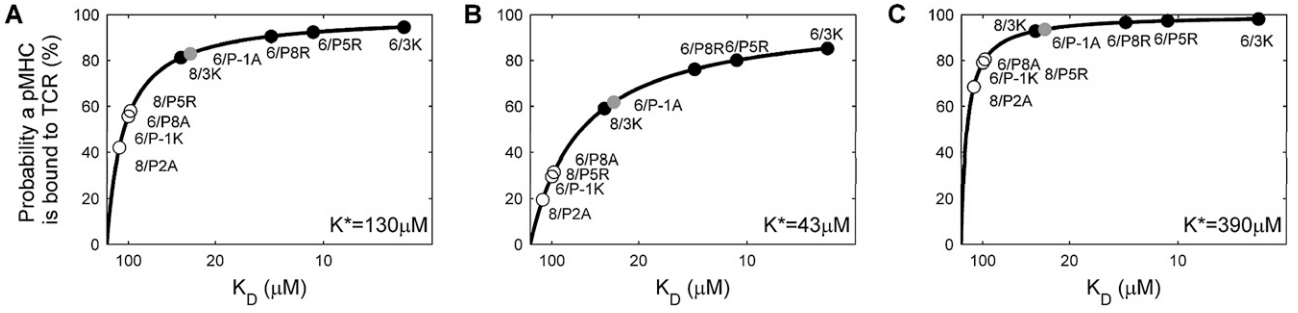

Fig. S6. Sensitivity of receptor occupancy to parameter estimates. The predicted receptor occupancy for each pMHC-TCR pair is plotted, according to Eq. **1**, using a K* of 130 μM as estimated in the main text (*A*) and with a K* three times stronger (43 μM) (*B*) and three times weaker (390 μM) (*C*). The different K*s model uncertainty in the concentration of TCRs on the surface of the cell and the conversion between SPR-measured affinities and affinities on the membrane.

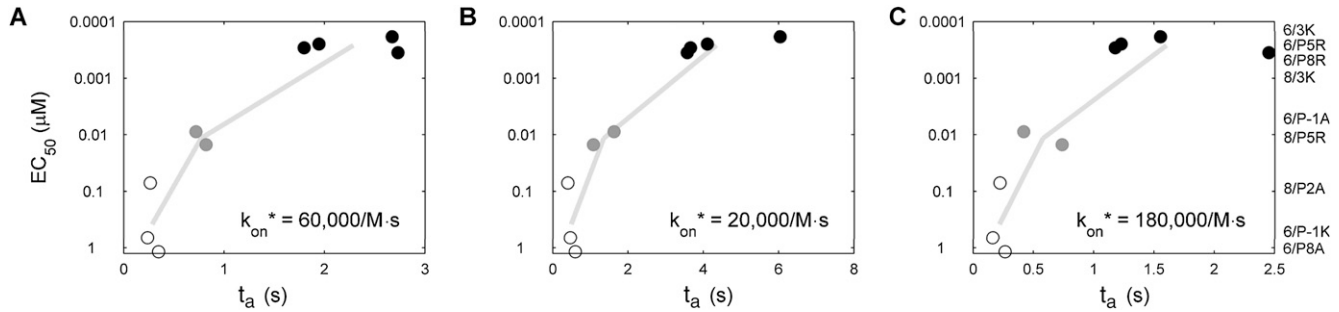

Fig. S7. Sensitivity of rebinding to parameter estimates. Correlations between peptide potency and the t_a are plotted with a rebinding threshold, k_{on}*, of 60,000/M·s (*A*), as estimated in the main text, and with rebinding thresholds three times lower (20,000/M·s) (*B*) and three times higher (180,000/M·s) (*C*). The t_as were determined according to Eq. **2**. The different rebinding thresholds model uncertainty in the diffusivities of the pMHCs and TCRs and the conversion between SPR-measured k_{on} and k_{on} on the membrane.

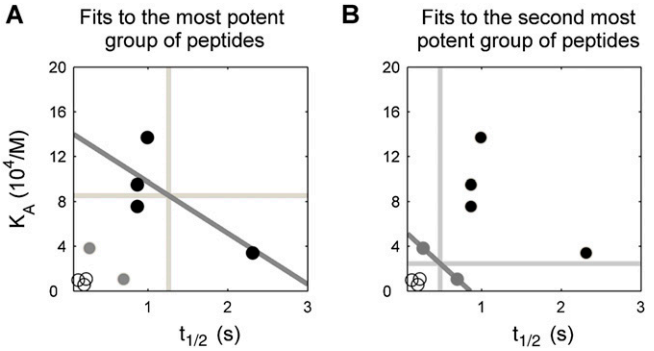

Fig. S8. Models are compared according to their ability to account for peptides with equal activity but different affinities, k_{on}, and $t_{1/2}$s. (*A*) Models are fit to the most potent group of peptides, which all have similar potency. The vertical, horizontal, and diagonal lines correspond to best-fits for the $t_{1/2}$, affinity, and rebinding models, respectively. (*B*) Models are fit to the second most potent group of peptides. The best-fits for the rebinding model correspond to rebinding thresholds, k_{on}^{*}, of 32,000/M·s (*A*) and 45,000/M·s (*B*). These are similar to the best-fits obtained using the techniques in Fig. S5.

Table S1. TCR-ligand K_D, binding kinetics, and T-cell effector functions

TCR	IA^b + 3K mutation	K_D (μM)	k_{on} (1/M·s)	k_{off} (1/s)	$t_{1/2}$ (s)	Proliferation EC_{50} (nM)	TNF-α EC_{50} (nM)
B3K506	WT	7	101,918	0.7	0.9	0.2	3.1
B3K506	P5R	11	74,654	0.8	0.9	0.2	6
B3K506	P8R	13	64,318	0.8	0.8	0.3	7
B3K506	P-1A	26	101,731	2.6	0.3	9	68
B3K506	P8A	92	33,370	3.1	0.2	1,200	2,210
B3K506	P-1K	101	55,149	5.6	0.1	660	5,500
B3K506	P8Q	114	ND	>5	<0.2	9,800	>10,000
B3K506	P-1L	122	ND	>5	<0.2	710	3,600
B3K506	P8L	256	ND	>5	<0.2	>10,000	>10,000
B3K506	P2A	278	ND	>5	<0.2	750	5,500
B3K506	P3A	>550	ND	ND	ND	>10,000	>10,000
B3K506	P5A	>550	ND	ND	ND	>10,000	>10,000
B3K506	P5Q	>550	ND	ND	ND	>10,000	>10,000
B3K508	WT	29	10,887	0.3	2.2	0.4	6
B3K508	P5R	93	11,048	1.0	0.7	15	87
B3K508	P2A	175	19,914	3.5	0.2	71	530
B3K508	P5A	>550	ND	ND	ND	5,700	>10,000
B3K508	P-1A	>550	ND	ND	ND	>10,000	>10,000
B3K508	P8R	>550	ND	ND	ND	980	>10,000
B3K508	P8A	>550	ND	ND	ND	>10,000	>10,000
B3K508	P3A	>550	ND	ND	ND	>10,000	>10,000

Scatchard analysis of binding data data were used to determine the dissociation constant (K_D). The k_{on} was calculated from the K_D and k_{off} ($k_{on} = k_{off}/K_D$). The $t_{1/2}$ values were calculated using first-order reaction kinetics: $t_{1/2} = \ln(2)/k_{off}$. ND, not determined.